The Skull of *Phyllomedusa sauvagii* (Anura, Hylidae)

MARIO R. RUIZ-MONACHESI,[1,2]* ESTEBAN O. LAVILLA,[1,2] AND RICARDO MONTERO[1,2,3]

[1]Instituto de Herpetología, Fundación Miguel Lillo, Miguel Lillo 205, S. M. de Tucumán, Tucumán, Argentina

[2]UEL - CONICET – Consejo Nacional de Investigaciones Científicas y Técnicas, Argentina

[3]Facultad de Ciencias Naturales, Universidad Nacional de Tucumán (UNT), Tucumán, Argentina

ABSTRACT

The hylid genus *Phyllomedusa* comprises charismatic frogs commonly known as monkey, leaf or green frogs, and is the most diverse genus of the subfamily Phyllomedusinae, including about 31 species. Although there is some information about the anatomy of these frogs, little is known about the osteology. Here the adult skull of *Phyllomedusa sauvagii*, both articulated and disarticulated, is described and the intraspecific variation is reported. Additionally, cartilage associated with the adult skull, such as the nasal capsules, auditory apparatus, and hyobranchial apparatus, are included in the analysis. Further examination of disarticulated bones reveals their remarkable complexity, specifically in the sphenethmoid and of the oocipital region. The description of disarticulated bones is useful for the identification of fossil remains as well as providing morphological characteristics that are phylogenetically informative. When comparing the skull morphology with the available information of other species of the genus, *Phyllomesusa sauvagii* skull resembles more that of *P. vaillantii* and *P. venusta* than *P. atelopoides*. Anat Rec, 00:000–000, 2016. © 2016 Wiley Periodicals, Inc.

Key words: Phyllomedusinae; anatomy; cartilages; chondrocranium

INTRODUCTION

The frog subfamily Phyllomedusinae comprises a group of charismatic species commonly known as monkey, leaf or green frogs, distributed from the tropical areas of Mexico to Central Argentina. It contains 60 species distributed in five genera, including *Agalychnis* (15), *Cruziohyla* (2), *Phasmahyla* (7), *Phrynomedusa* (5), and *Phyllomedusa* (31) (Frost, 2015). They have numerous reproductive, behavioral, biochemical, and morphological features that clearly distinguish them from other members of the family Hylidae, and its monophyly is supported by numerous molecular and morphological characters, both adults and larvae (Faivovich et al., 2010). The subfamily has been the focus of several taxonomic and systematic studies (e.g., Funkhouser, 1957; Wiens et al., 2005, 2006; Gomez-Mestre et al., 2008; Faivovich et al., 2010; Wiens et al., 2010; Pyron and Wiens, 2011), but our current understanding of the phylogenetic relationships of Phyllomedusinae is based mainly on the analysis of molecular data. Unfortunately, the phylogenetic utility of morphological characteristics of the group has not yet been thoroughly explored, being the osteological descriptions scarce, with the contributions by Duellman (1970), Cannatella (1980),

Grant sponsors: CONICET; Grant number: PIP-CONICET 112 200801 02422; Grant sponsor: Universidad Nacional de Tucumán; Grant numbers: CIUNT G430 and PIUNT G519.

*Correspondence to: Mario R. Ruiz-Monachesi, Miguel Lillo 251-CP 4000, Tucumán, Argentina. E-mail: kobe_mar13@hotmail.com

Received 20 May 2015; Revised 4 August 2015; Accepted 23 December 2015.

DOI 10.1002/ar.23331

Published online 00 Month 2016 in Wiley Online Library (wileyonlinelibrary.com).

da Cruz (1990), and Sheil and Alamillo (2005) as the most noticeable exceptions.

Phyllomedusa is the most diverse genus within the subfamily, and was the focus of numerous studies related to reproduction and mating behavior, physiology, biochemistry of the nitrogen cycle, skin histology and histochemistry, characterization of bioactive secretions, and so on, exhaustively reviewed in Faivovich et al. (2010). Despite the diversity of the genus, there are osteological information for only two Peruvian species, *Phyllomedusa vaillantii* and *P. atelopoides* (Sheil and Alamillo, 2005), along with a general description of the skull of the meridional *P. venusta* (Duellman, 1970; Cannatella, 1980).

To make comparisons among species (for morphological, morphofunctional, or phylogenetic studies), it is necessary to have a good starting point (i.e., a detailed description of at least one species), and this is the main goal of this article. In fact, studies of individual bones of the anuran skull are scarce, in contrast to descriptions of postcranial osteology that frequently concentrate on individual elements (such as the humerus or femur) or on units such as the pelvic girdle (e.g., Felix and Montori, 1986). Information detailing disarticulated cranial elements would be useful for paleontologists or neonatologists identifying individual bones or bone fragments in sediment or stomach contents. Moreover, the complex architecture of several bones is hidden in articulated skulls (Montero and Gans, 1999; Conrad, 2004); thus potentially informative phylogenetical characters may be overlooked.

This contribution provides a detailed osteological description, including both articulated and disarticulated cranial bones, of *Phyllomedusa sauvagii* Boulenger, 1882, a species distributed in Argentina, Bolivia, Brazil, and Paraguay. It also explores the cartilaginous elements of the adult head, which have been described for less than 1% of all anuran species, including *Phyllomedusa vaillantii* and *P. atelopoides* (Sheil and Alamillo, 2005). The study, we hope, will enrich the scant available information on *Phyllomedusa* (and on anurans in general) osteology, as a starting point for further anatomical and phylogenetic research.

MATERIALS AND METHODS

Nineteen specimens of *Phyllomedusa sauvagii* were examined for this study (13 males and 6 females; Appendix 1). Of these, 12 were complete dry skulls, 5 were cleared-and-double-stained specimens, and 2 were disarticulated dried skulls. Dried skulls were prepared by removing the flesh by hand and cleaning the skulls in a commercial bleach solution. The cleared-and-double-stained specimens were prepared following the protocol of Wassersug (1976). The skulls were disarticulated by soaking them in tap water for several weeks until the bones separated. The osteological terminology follows that of Trueb (1973, 1993), Sanchíz (1998), Sheil and Alamillo (2005), and Barrionuevo (2013). The terminology for cartilages follows that of Pugener and Maglia (2007). From the ethical standpoint, *Phyllomedusa sauvagii* was considered a Least Concen (LC) species in the IUCN Amphibian redlist (Aquino et al., 2015) and in the last categorization of Argentinean amphibians (Vaira et al., 2012).

RESULTS

Articulated Skull

The skull is high, longer than wide (width/length = 0.78), lacks obvious ornamentation, and has a narrow, elongated and subrectangular frontoparietal fontanelle. In dorsal view (Fig. 1A), the shape of the skull is approximately trapezoidal. The maxilla bears a high pars facialis that extends dorsally up to the level of the neopalatine. Each nasal bone covers about half of the olfactory capsule; the bones are usually narrowly separated at midline, and are either posteriorly separated from, or in contact with, the sphenethmoid. In lateral view, the skull is also trapezoid shaped, with the ventral edge straight and the dorsal edge rounded anteriorly and straight posteriorly. The squamosals are moderately developed, with a long otic ramus and a short zygomatic ramus that extends no more than one-third the distance to the maxilla. The quadratojugals are slender. The alary processes of the premaxillaries extend dorsally and posteriorly. In ventral view, the sphenethmoid is wide and short; the dentigerous processes of the vomer are dentate, oriented at a slight angle or perpendicular to the midline. The pterygoids are slender and are connected with the prootics through a narrow, lateral cartilaginous band. The otic region has a quadrangular shape. Teeth are present on the premaxilla and the maxilla, and have almost spherical tips.

The skulls of adult females are usually larger than those of males. The key distinction is skull width, which results in a different lateral angulation of the pterygoids. In the wider female skull, the posterior ramus of the pterygoids are oriented more posterolaterally than in males. The snout of females is also more rounded than the more truncated snout of males. Furthermore, the maxillae are bent laterally in females, whereas they are straighter in males.

Individual Bones

Snout. *Nasal Capsules.* The cartilages of the snout (Fig. 2) are arranged into an anterior group, those that form the anterior wall of the nasal capsules, and a posterior group that forms the posterior wall of the nasal capsules and the anterior border of the orbit; both groups are joined by the septum nasi.

The cartilages of the anterior group form a wide ventral plate (the solum nasi; not illustrated) and a wide dorsal plate (the tectum nasi). The tectum covers the nasal cavities and bears several cartilages and crests. Posteriorly, the tectum nasi is very narrow, barely covering the septum nasi, a vertical cartilaginous plate on the saggital plane that separates the nasal cavities. Anteriorly, the tectum nasi is much wider, extending between the nares. The lateral extensions of the tectum are the oblique cartilages that form the dorsal edge of the nares. Anteriorly there are two rami of prenasal cartilages, the superior and the inferior prenasal cartilages. The inferior (ventral) prenasal cartilage is an extension of the solum nasi, and is present as a long, slender cartilaginous bar that extends distally, and is parallel to the border of the alary process of the premaxilla until it contacts the premaxillary pars dentalis. The superior (dorsal) prenasal cartilage is an anterior process of the tectum nasi; it is shorter than the inferior process and its distal tip contacts the dorsal margin of the pars alaris of the premaxilla. The margins of the nares are formed by the alary cartilage, the crista subnasalis, the cartilaginous

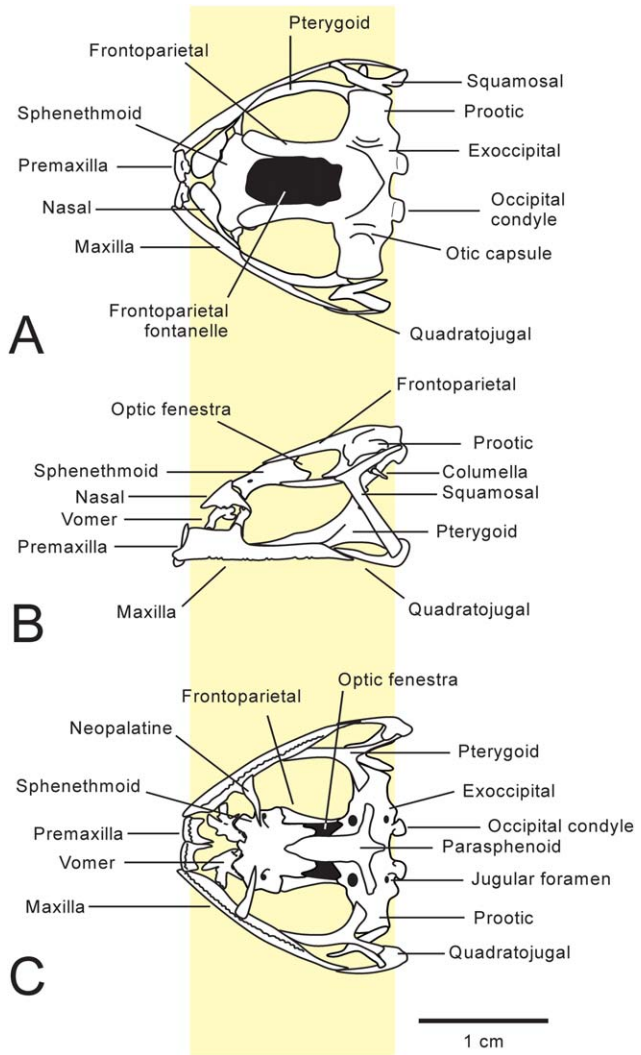

Fig. 1. Skull of *Phyllomedusa sauvagii*: (**A**) dorsal, (**B**) lateral, and (**C**) ventral views.

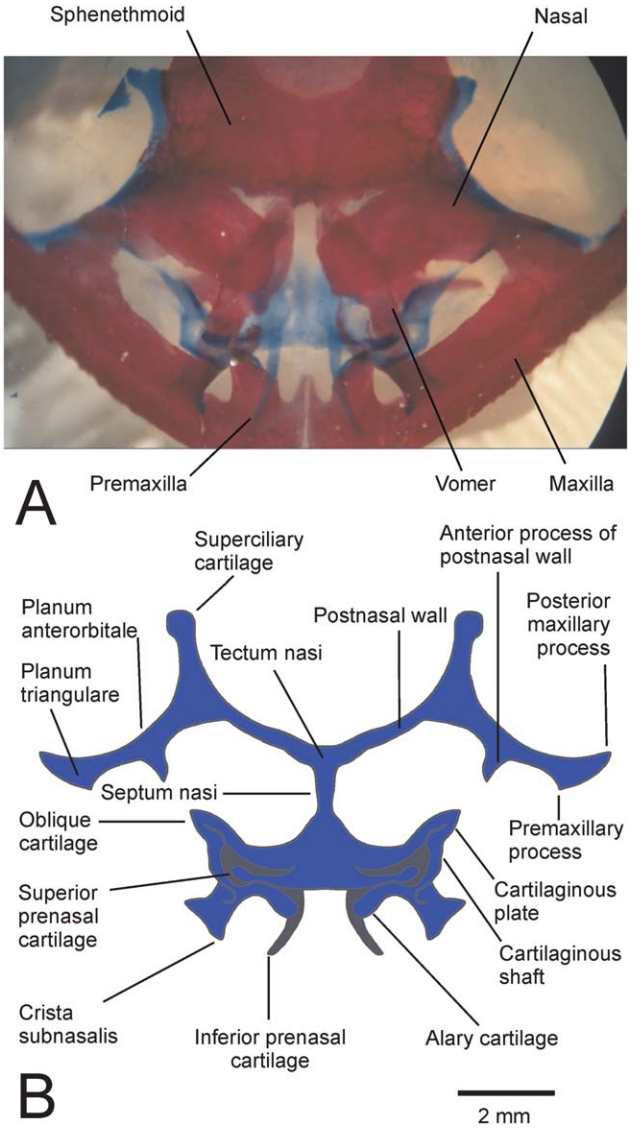

Fig. 2. Dorsal view of the nasal capsule of *Phyllomedusa sauvagii* (FML 25331). Anterior to the bottom. (**A**) Double-stained specimen in which the bone is red stained and the cartilague is blue stained; some bones are labeled for orientation.

shaft, and the cartilaginous plate. The alary cartilage is anterior to the superior prenasal cartilage and of approximately equivalent size; it forms the anterior edge of the nares and contacts the dentigerous process of the vomer. The crista subnasalis projects laterally from the solum nasi; its distal tip is truncated and its border is approximately parallel to the dorsal edge of the pars facialis of the maxilla. There is a cartilaginous shaft that connects the anterior crista subnasalis with a wide, subtriangular planum terminale (not illustrated).

The cartilages of the posterior group form the postnasal wall, a plate that extends perpendicular to the sagittal plane, separating the nasal capsules from the orbits. The lateral (distal) extreme of the postnasal wall, the planum triangulare, is narrow and subtriangular in shape in dorsal view. It attaches to the posterior edge of the neopalatine process of the maxilla. The anterior premaxillary process is short and projects slightly beyond the tip of the palatine process, to the lateral edge of the nasal. Dorsally, there is a superciliar cartilage, a process that borders the dorsal edge of the orbit.

Premaxilla. The premaxillae are paired, each having a horizontal base that bear teeth (pars dentalis), a posterior laterally projecting lamina (pars palatina), and a prominent dorsal or alary process (pars alaris) (Fig. 3).

The alary process (pars alaris) is a lamina that projects dorsally and is posteriorly concave. When viewed laterally, the alary process of each premaxilla has a dorsal and slightly posterior orientation in relation to the ventral border of the skull (Figs. 1B, 3B). In frontal view (Fig. 3A), the alary process is vertical and parallel to its contralateral process. The terminus of the alary process is blunt, in contact with the alary cartilage of the nasal capsule (Fig. 2), and is directed toward the nasal bone.

The ventral border of the par dentalis is horizontal and continuous with that of the pars dentalis of the maxilla. The pars dentalis bears 11–15 pedicellate teeth, which are

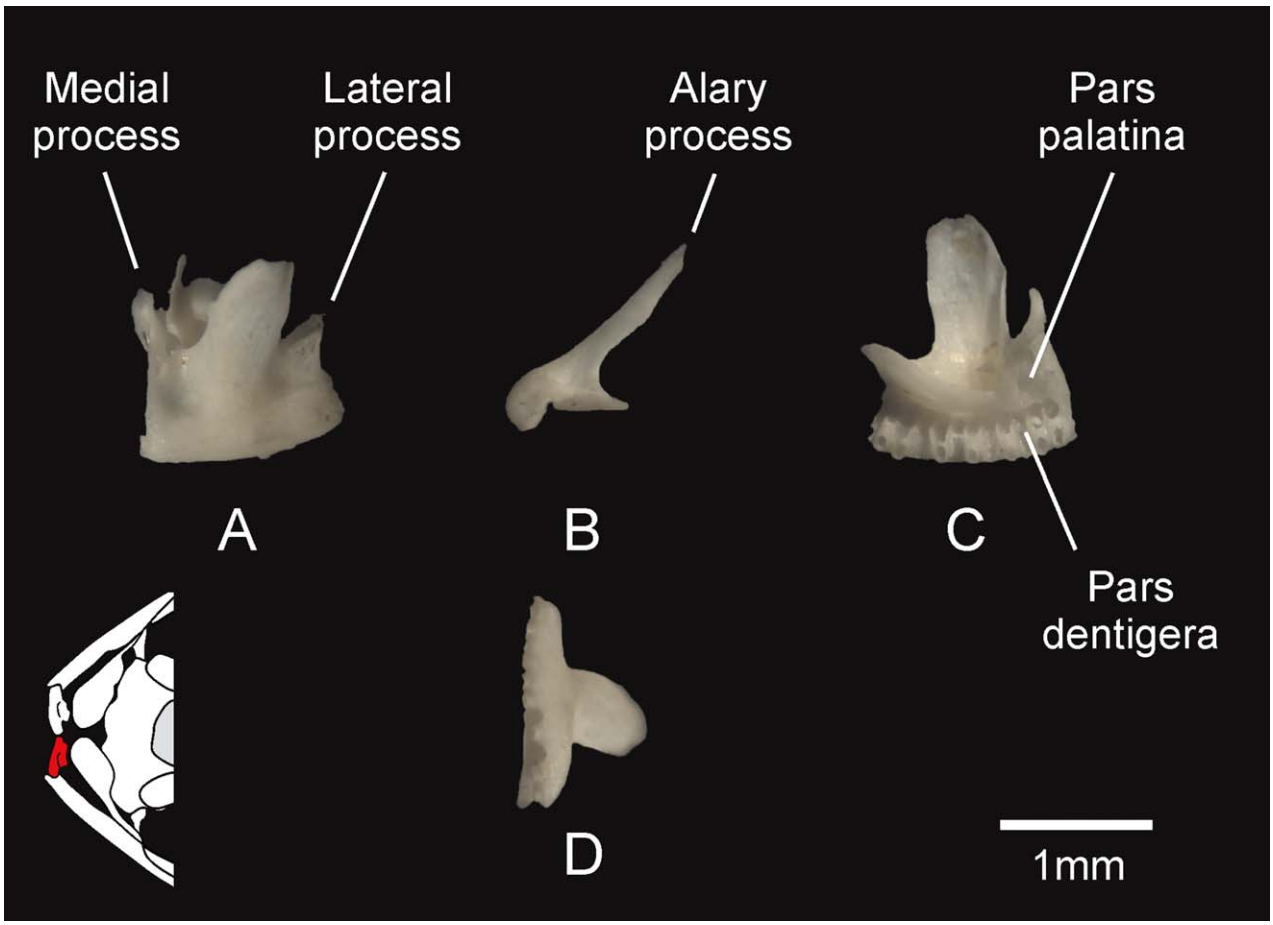

Fig. 3. Left premaxilla of *Phyllomedusa sauvagii*: (**A**) dorsal, (B) lateral, (C) ventral, and (D) anterior views.

slightly curved and have globular distal tips. The pars dentalis extends ventrally more than the pars palatina, a characteristic clearly noted in lateral view (Fig. 3B).

The pars palatina projects posteriorly on the medial and lateral sides of the pars alaris, and has two posterior processes—the posteromedial and posterolateral processes (Fig. 3A). The posteromedial process is approximately twice as long as the posterolateral one. The posterolateral process of the premaxilla has very loose contact with the anterior rostrum of the maxilla.

In the articulated skulls of females, the ventral margin of the pars dentalis of the premaxilla is at the same level as that of the maxilla, giving the maxillar arcade a flat border. In males, the pars dentalis is more ventrally positioned than the maxilla, giving the skull a more undulating maxillar arcade.

Septomaxilla. The septomaxilla is a tiny, paired bone, encapsulated within the cartilages of the nasal capsule and thereby having no articulation with other bones. As this minuscule bone is usually lost during dry skull preparation, it was studied on cleared specimens. The septomaxilla is located posterior to the pars alaris of the premaxilla and anterior to the sphenethmoid, ventral to the nasal, and dorsal to the vomer. It is triradiate, with two posterior processes and a smaller anterolateral process (Fig. 4).

Nasal. This trapezoidal bone has a complex curvature (Fig. 5) as it overlies the nasal capsule dorsally. Its major axis is tilted anteriorly toward the sagittal plane, at which point it nears its contralateral without contacting it (Fig. 1). The posterior edge of the bone articulates with the sphenethmoid. Laterally, it exhibits a long, pointed paraorbital process, which is angled toward the orbit; this process overlaps dorsally with the superciliar cartilage and comes in contact with the neopalatine. The anterior edge of the bone is irregular and, on its middle region, there is a dentate and short ventrally facing parachoanal process.

Vomer. Each vomer lies ventral to the cartilages of the olfactory capsule and has articulates laterally with the maxilla and dorsoposteriorly with the sphenethmoid. The paired vomers do not articulate medially and each bears four divergent processes (Fig. 6): anterior, prechoanal, postchoanal, and dentigerous processes. In dorsal view (Fig. 6B), the bone is K-shaped, with the main axis formed by the anterior and posterior dentigerous processes, and laterally by the prechoanal and postchoanal processes. The medial border of the main axis of the K forms a thin lamina, which bears a short denticulate projection at its midpoint; on the ventral side, the bone is creased and has a central concavity. In ventral view (Fig. 6A), three processes are visible, whereas the posterior dentigerous process is hidden

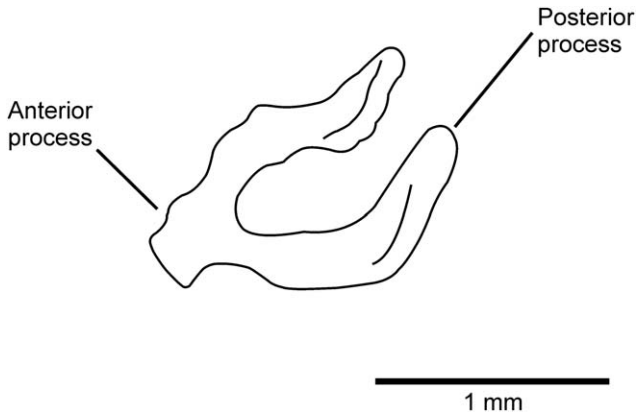

Fig. 4. Ventral view of the right septomaxilla of *Phyllomedusa sauvagii*. Anterior to the left.

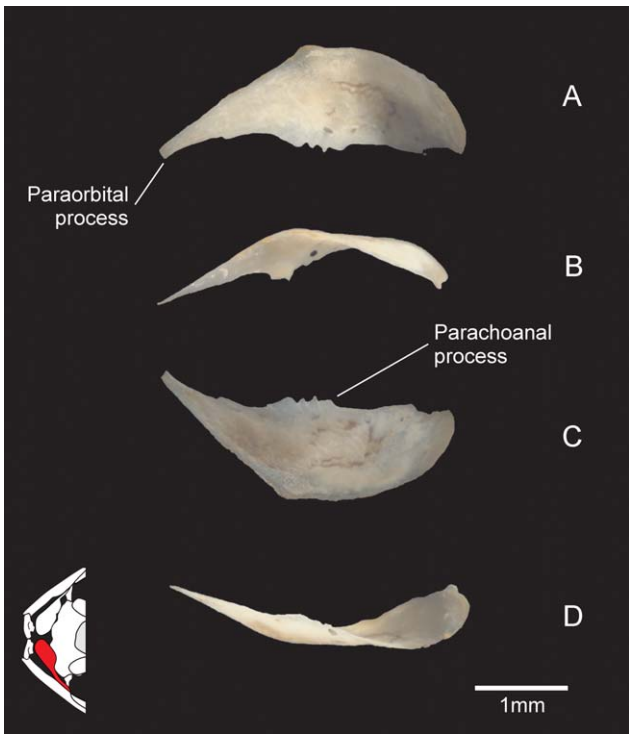

Fig. 5. Left nasal of *Phyllomedusa sauvagii*: (**A**) ventral, (**B**) posterior, (**C**) dorsal, and (**D**) anterior views. Lateral to the left.

by the medial lamina. The anterior process is the longest and extends nearly to the premaxilla–maxilla suture; the margins of the process are irregular. The prechonal process articulates laterally with the pars facialis of the maxilla. The postchoanal process is shorter than the prechoanal process; it has a sharp tip that lies between the ventral margin of the nasal and the dorsal margin of the sphenethmoid trabeculum. The dentigerous process bears 2–6 pedicelate teeth, and its tip contacts the ventral margin of the sphenethmoid trabeculum.

Neopalatine. This rod-like bone is paired and connects the sphenethmoid with the maxilla (Fig. 1C). The medial termius articulates with the sphenethmoid, can be sharp or

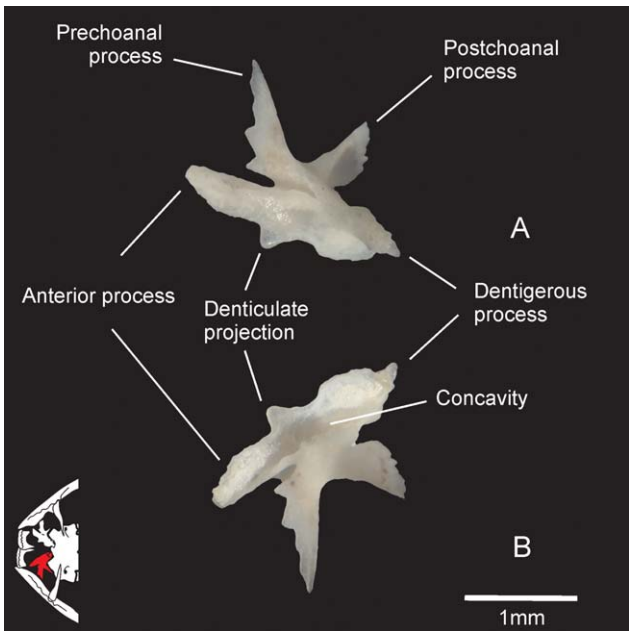

Fig. 6. Left vomer of *Phyllomedusa sauvagii*: (**A**) ventral and (**B**) dorsal views. Anterior to the left.

acuminate. The lateral terminus, which articulates with the maxilla, is blunt. According to Cannatella (1985) and Trueb (1993), this bone is not homologous to the other tetrapod palatine and represents a neoformation of neobatrachians.

Circumorbital region. *Sphenethmoid.* This azygous, wide bone is located at the center of the anterior half of the skull (Fig. 1), positioned between the braincase and the nasal capsules. The sphenethmoid forms the anterior limit of the braincase and the anteromedial edge of the orbit; dorsally it delineates the frontoparietal fontanelle (Fig. 1A) and, laterally, the optic fenestra (Fig. 1B).

The flat dorsal surface is invested anteriorly by the nasals and posteriorly by the frontoparietal; the ventral surface is flat anteriorly but concave posteriorly, and contacts the vomers anteriorly, the neopalatines laterally, and the cultriform process of the parasphenoid posteriorly.

The anterior edge of the sphenethmoid is straight in dorsal view (Fig. 7D and E). The anterior edge of its ventral face bears three blunt processes; the central process is smaller than the lateral processes, which diverge somewhat laterally (Fig. 7). The dentigerous process of the vomer is set between the central processes, whereas the postchoanal process of the vomer overlaps (dorsally) with the anterior edge of each trabecula (i.e., lateral processes). The posterior border of the ventral face of the sphenethmoid is extensively invested by the distal tip of the cultrifom process of the parasphenoid (Fig. 1C). The lateral face of the sphenethmoid ends posteriorly in a concave border, which forms the anterior boundary of the optic fenestra. Located on the posterior end of the sphenethmoid are a pair of narrow cartilaginous strips (remmants of the floor of the larval chondrocranium) that border laterally the cultriform process.

The disarticulate sphenoethmoid (Fig. 7) reveals a complexity not demonstrated in the articulate skull. Between the ventral and dorsal faces, the bone is hollow. Anteriorly,

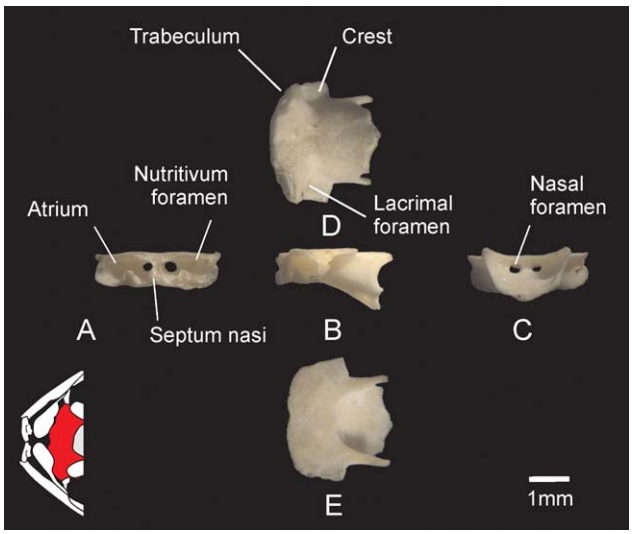

Fig. 7. Sphenoethmoid of *Phyllomedusa sauvagii*: (**A**) anterior, (**B**) left lateral, (**C**) posterior, (**D**) ventral, and (**E**) dorsal views. In B, D, and E, anterior to the left.

there is a pair of cavities, the olfactory atria, divided medially by the septum nasi, whereas posteriorly, the bone forms an atrium that contains the olfactory lobes of the brain. In the posterior wall of each atrium, near the sagittal plane, there is a nasal foramen for the passage of the olfatory nerve. Offset laterally in the same posterior wall, a smaller nutritivum foramen (sensu Estes and Reig, 1973). The posterior atrium is a broad cavity with a dorsal ceiling that is formed by the cartilage that closes the frontoparietal fontanelle; laterally, two posterodorsal processes delimit the fontanelle and divide the wide cavity.

Maxilla. The paired maxillae are elongated and curved, spanning most of the length of the maxillary arcade (Fig. 8). Each bone bears three regions: pars facialis, pars palatina, and pars dentalis. The pars facialis, defining the ventral perimeter of the orbit, is a vertical lamina in which the anterior region is taller than the posterior one. The pars palatina (Fig. 8D) is a narrow lamina that projects, at an acute angle, dorsomedially from the pars fascialis. Finally, the pars dentalis (Fig. 8C and D) is narrow and runs ventrally along the complete length of the bone, bearing 48–82 teeth. The pedicellate teeth have round cusps, whereas the pedicels have a slight concavity on the lingual side. The large nutritive foramina at the base of each tooth may support the buds for replacement teeth. The crowns of the teeth are rounded, with their edges slightly dentate.

In lateral view (Fig. 8B), the anterior region of the pars facialis is high and the dorsal border either straight or undulating. At approximately one-third of its length, the preorbital process projects slightly dorsally, and supports the lateral portion of the cartilaginous planum anteorbitale (Fig. 2). The process is straight and slender, and laterally overlaps the neopalatine, which cannot be seen in dorsal and lateral views of the skull. Posteriorly, the pars facialis becomes gradually smaller, shaping the anteroventral border of the orbit.

The pars palatina extends from the anterior tip of the maxilla to the base of its posterior process. The anterior third is wide but narrows slightly at the level of the preorbital process, whereas the rear part of this structure maintains its width, until it abruptly ends, abutting the anterior process of the pterygoid. Some portions of the chondrocranium abutts on the pars palatina: anteriorly the crista subnasalis, and posteriorly the planum triangulare (Fig. 2).

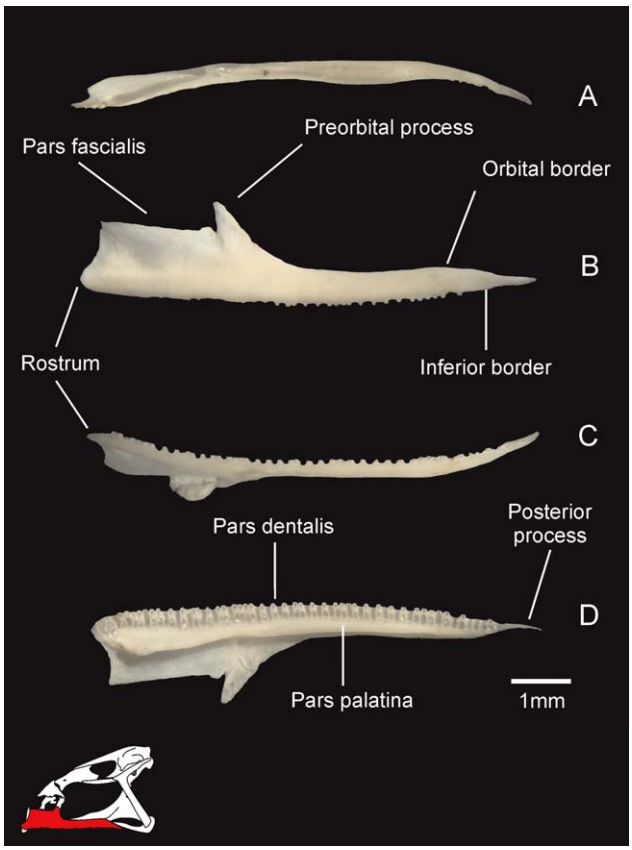

Fig. 8. Left maxilla of *Phyllomedusa sauvagii*: (**A**) dorsal, (**B**) lateral, (**C**) ventral, and (**D**) medial views. Anterior to the left. Due to the use of bleach during preparation of dried skulls specimens, only the hollow pedicels remain, with an apical hole where the crowns were attached.

Pterygoid. This is a triradiate, Y-shaped bone, located on the ventral face of the skull. Its rami (anterior, medial, and posterior) are oriented in different planes, giving this bone a complex configuration (Fig. 9). The tips of the anterior and posterior rami are acuminate, whereas the tip of the medial ramus is truncated. The anterior ramus is the longest, bearing a pterygoid furrow on its lateral face, which houses pterygoid process of the pars palatina of the maxilla. The medial ramus is the shortest (approximately half the length of the anterior ramus) and is directed slightly dorsomedial in order to articulate with the prootic. The anterior and medial rami form the margo orbitalis (Fig. 9C). Between the anterior and posterior rami is a thin, ventral lamina that has a wide lateral furrow, which is the articular surface for the ventral ramus of the squamosal. The posterior ramus articulates with the ventral ramus of the squamosal and the quadratojugal.

Braincase. *Occipital complex.* The posterior part of the adult skull is formed by a unique complex,

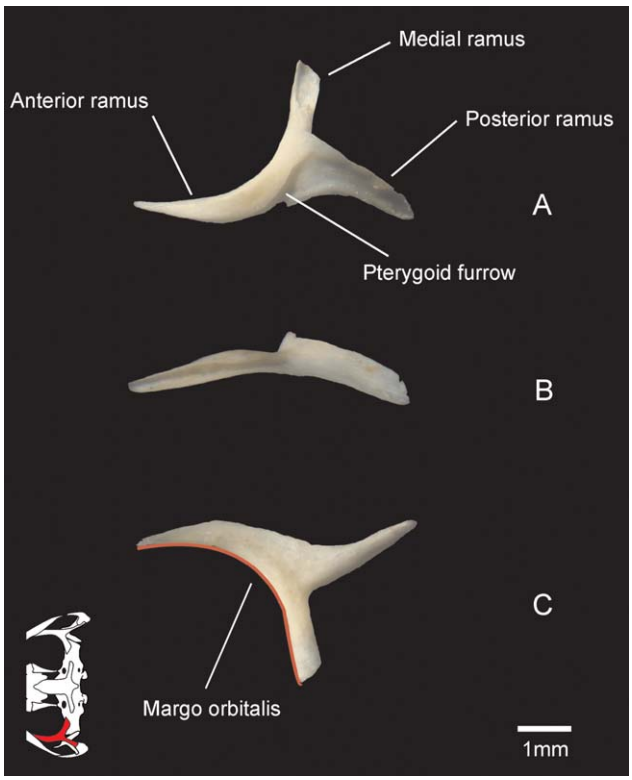

Fig. 9. Left pterygoid of *Phyllomedusa sauvagii*: (**A**) dorsolateral, (**B**) ventrolateral, and (**C**) ventromedial views. The red line indicates the orbital border (margo orbitalis). Anterior to the left.

which is the result of the fusion of several bones, including the frontoparietal, exoccipitals, and prootics (Fig. 10) (as in other *Phyllomedusa* species reported by Haas, 1996; de Sá and Lavilla, 1996; Sheil and Alamillo, 2005). There are no clear limits among the bones that comprise this complex. The only exception may be the dorsal area of the foramen magnum that exhibits a slope (but not clear suture), which we consider as the presumptive contact between the frontoparietal and exoccipitals. Therefore, as we cannot describe individual bones, we refer to their presumptive areas: frontoparietal, prootic, and exoccipital areas.

The frontoparietal area is U-shaped, with a pair of anteriorly oriented arms (the frontal portion) and a triangular base (the parietal portion); the space between the two frontal rami delimits an oval frontoparietal fontanelle that is closed anteriorly by the sphenethmoid (Fig. 1A). The bony border of the fontanelle is very thin and supports a thin connective sheet that closes the opening, forming the roof of the cranial cavity. The paired frontal processes are relatively thin laminas (with a slight curvature laterally and ventrally; Fig. 10E), whose blunt and slightly divergent termini overlap the sphenethmoid. Their concave lateral border shape is the dorsomedial margin of the orbit. The posterior medial area (the parietal portion) forms the roof of the cranial cavity and its ventral surface is concave (Fig. 11). The triangular parietal portion is elevated in relation to the prootic area, and posteriorly it reaches just dorsal of the foramen magnum.

The prootic area is a complex region of the skull; the lateral region of the back of the skull comprises the osseus crista parotica and the otic capsules. Its dorsal surface is smooth and quadrangular, with the anterior and posterior edges curved, and a convex lateral border. Flanking the frontoparietal area are two noticeable crests, divergent at a 90° angle, that indicate the semicircular channels of the inner ear (Fig. 10D). Although the anterior crest protrudes only slightly over the orbit, the posterior one protrudes markedly on the posterior wall of the skull (Fig. 10C) as it is approximately parallel to the lateral edges of the foramen magnum. On the posterior face of the skull, there is a wide jugular foramen, located between the occipital condile and the posterior semicircular crest. The crista parotica articulates anterolaterally with the otic process of the squamosal through a thin cartilaginous strip. On the lateral wall of the bone, slightly ventral to the crista parotica, opens the large, circular fenestra ovalis (Fig. 10E). The concave, smooth medial wall of the otic capsule (Fig. 11) is pierced by three aligned foramina beginning at the ventral angle formed by the intersection of the otic capsule with the exoccipital ventral plate. Through these foramina, the cranial nerves VII (facial), IX (glossopharyngeal), and X (vagus) exit the cranium; the foramina sizes increase anteriorly to posteriorly (homology of the foramina according to Bellairs and Kamal, 1981). Dorsal to the above mentioned is the endolinfatic foramen, which communicates the inner ear with the cranial cavity. Anteriorly, there is a large prootic foramen (Fig. 10A; Fig. 11) to allow the passage of the gasserian ganglium of the trigeminum cranial nerve.

The area of the exoccipitals surrounds a wide, pentagonal shaped foramen magnum, whose dorsal angle is just ventral of the parietal area; the ventral border, between the condyles, is straight. Each paired occipital condyle has a marked base or neck, and a distal, semispherical, rounded head. Ventrally, the exoccipitals form a wide plate that laterally is continuous with the ventral regions of otoccipital (Fig. 10E). Anteriorly, the plate has a groove-like recess (Fig. 10E), to accommodate the posterior tip of the parasphenoid.

Parasphenoid. The parasphenoid is cross-shaped and unornamented (Fig. 12). The long, wide anterior cultriforme process overlaps the posterior one-third of the sphenethmoid. The lateral alary processes of the parasphenoid are narrow and extend toward the medial ramus of the pterygoid without contacting it. The posteromedial tip of the parasphenoid projects to the ventral edge of the foramen magnum. The dorsal face of the parasphenoid (Fig. 12B), hidden in the articulated skull, is concave.

Suspensorium. *Quadratojugal.* This bone contacts the posterior terminus of the maxilla, the squamosal, and the pterygoids, forms the lateral border of the parietal fenestra, and articulates with the mandible. The anterior extreme is sharpened (the maxillary process), with a wide posterior expansion (the quadrate portion) (Fig. 13B). The articulation of the maxillary process bevels with the posterior process of the maxilla and typically overlaps one-third to one-half of the quadratojugal length. The quadrate portion is dorsomedially oriented, and therefore, the bone in its physiological position does not show most of the main characteristics;

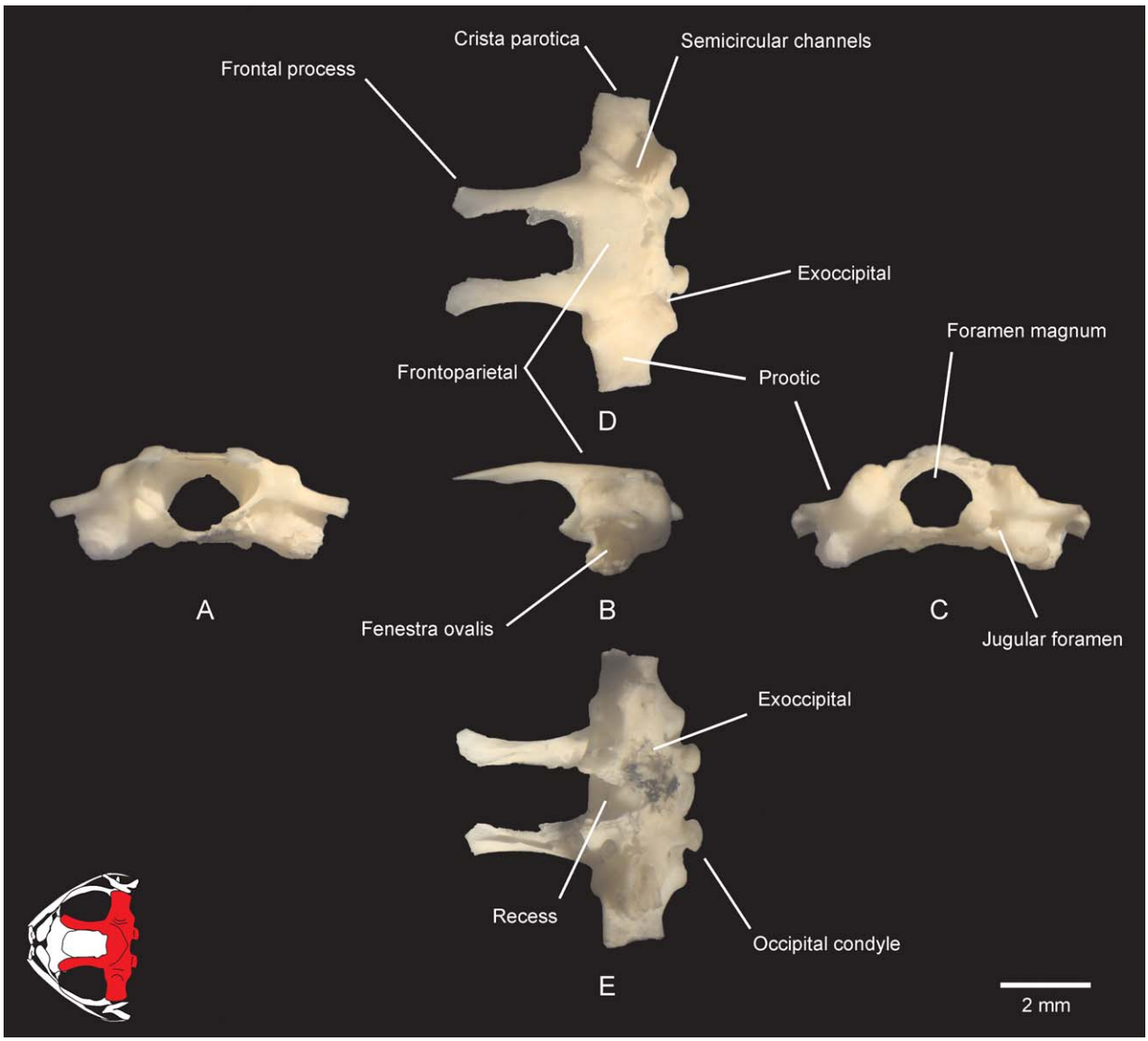

Fig. 10. Occipital complex of *Phyllomedusa sauvagii*: (**A**) anterior, (**B**) lateral, (**C**) posterior, (**D**) dorsal, and (**E**) ventral views. In B, D, and E, anterior to the left.

for that reasons, the views of Figure 13 are not orthogonal to the physiological position, but to the main surfaces of the bone. The posterior face of the quadrate portion is covered by a cartilaginous cap that articulates with the mandible (Fig. 13D). The distal tip of the ventral ramus of the squamosal articulates with the dorsolateral face of the quadrate area (Fig. 13C), whereas the posterior ramus of the pterygoid articulates with the ventromedial surface of the quadrate area (Fig. 13A). The three surfaces that articulate with the squamosal, pterygoid, and mandible are concave.

Squamosal. The T-shaped squamosal joins the neurocranium with the quadratojugal and maxillary arcade. It bears three rami: posterior (otic), ventral, and anterior (zygomatic) (Fig. 14). Comparatively in lateral view, the anterior ramus is about one-half the length of the posterior one, and the posterior is about one-fourth of the length of the ventral ramus. The posterior ramus articulates with the paroccipital process of the otic capsule. The ventral ramus is the longest and has a slight posterior orientation; it articulates medially with the squamosal and the quadratojugal; on the lateral surface of the ventral process, there is a flat, or slightly concave, surface (possibly for muscle attachment). Along the bases of the dorsal and ventral processes, there is the lamina alaris that is curved. The reduced anterior ramus has an anteroventral—and slightly lateral—orientation, and bears a sharp tip that does not contact any other bone.

Auditory apparatus. The tympanum is supported by a chondral tympanic annulus, which is located lateral

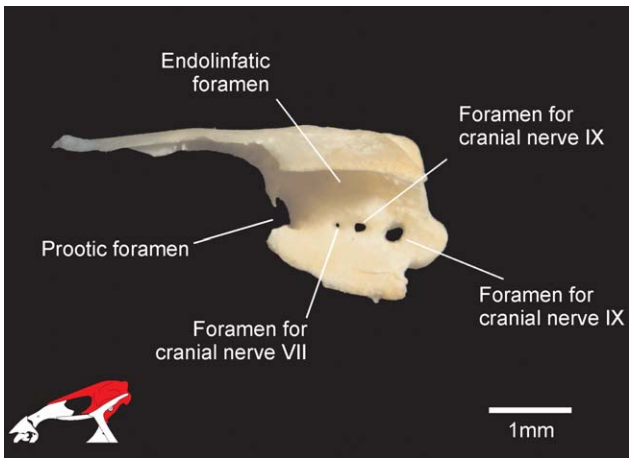

Fig. 11. Medial view of occipital complex of *Phyllomedusa sauvagii*. The bone was cut in the midline to reveal this view. Anterior to the left.

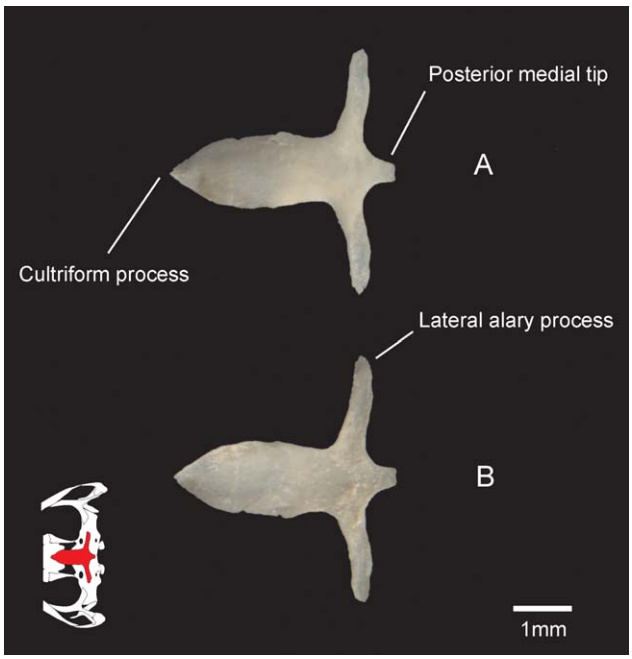

Fig. 12. Parasphenoid of *Phyllomedusa sauvagii*: (**A**) ventral and (**B**) dorsal views. Anterior to the left.

to the squamosal (Fig. 15). It has the shape of an incomplete dorsally opened ring; the inner border is thicker than the outer.

The columella is a well ossified element formed by the pars interna plectri (which forms the short basal plate of the columella that occludes most of the fenestra ovalis), fused synostotically with the pars media plectri (the osseous shaft that bridges the middle ear), and the pars externa plectri or extracolumella (a thin cartilaginous bar that connects the distal tip of the columella with the tympanic membrane, that is, half the length of the pars media). Near the putative limit between the basal plate and the shaft, the columella is perforated by a tiny stapedial foramen, presumably for the passage of the stapedial artery (Fig. 16B). The quadrangular, cartilaginous operculum closes the aperture of the fenestra ovalis, located slightly posterior to the basal plate of the columella.

Mandible. Each ramus of the slender, edentate mandible (Fig. 17) is sigmoid-shaped; its lateral side is posteriorly concave and anteriorly convex. From posterior to anterior, the mandibular bones are: a large angulosplenial, a reduced dentary, and a small mentomecklian cartilage.

Angulosplenial. The sigmoid angulosplenial is the principal bone forming the mandible (Fig. 18). The posterior region has a labial concavity, whereas the longer anterior region has a lingual concavity; the curvature changes at the level of the coronoid process, which is located approximately one-quarter of the length from the posterior end. The coronoid process is dorsomedial, short and compressed process, oriented slightly posteriorly, and forms the site of insertion for the adductor muscles of the mandible attach. The entire length of the medial surface is surcated by a deep Meckel's groove, to accommodate Meckel's cartilage; the groove is dorsolateral, proximally, and becomes lateral distally. Whereas the angulosplenial is cylindrical posteriorly, anteriorly it becomes higher and compressed. The anterior tip of the angulosplenial is truncated and does not contact the mentomekelian, which is separated by a connective pad. Meckel's cartilage broadens, proximally, dorsal to the angulosplenial; the cartilage forms a dorsal cup that embraces the quadratojugal, forming the articulation of the mandible. At the level of the coronoid process, Meckel's cartilage switches from the dorsal to the lateral surface of the angulosplenial and narrow slightly. Anteriorly, the cartilage broadens to the height of the mandible, and extends beyond the terminus of the angulosplenial to articulate with the mineralized mentomeckelian cartilage.

Dentary. The dentary (Fig. 19) is a thin, weakly-ossified bone that laterally closes the anterior part of the Meckel's groove. Anteriorly the dentary is taller and concave, and on the labial side, it overlaps the mentomakelian almost to the medial border, where they fuse; posteriorly, the dentary is flat and pointed, extending to the middle of the angulosplenial. The dentary is so thin that it is flexible and is often lost or damaged during the preparation of dry skulls. Likewise, in cleared-and-stained specimens, this bone can be so weakly stained by the Alizarine that it is diffucult to observe next to Meckel's cartilage when *in situ*.

Mentomeckelian. The mentomeckelian (Fig. 20) is short and each articulates at the midline with its neighbor by synchondrosis. The posterior terminus of the mentomeckelian is separated from the angulosplenial by a connective pad. The mentomeckelian is invested laterally by the anterior tip of the dentary bone, partially fusing with it; in Fig. 20, the mentomeckelian still has the broken tip of the dentary. The medial end of the mentomeckelian is attached to its counterpart by a strong ligament; it has a dorsoposterior process that projects like a median "tooth." In the medial (distal) view (Fig. 20E), a hollow cavity is evident, at the bottom of which there is a foramen possibly for the attachment of the simphysial ligaments.

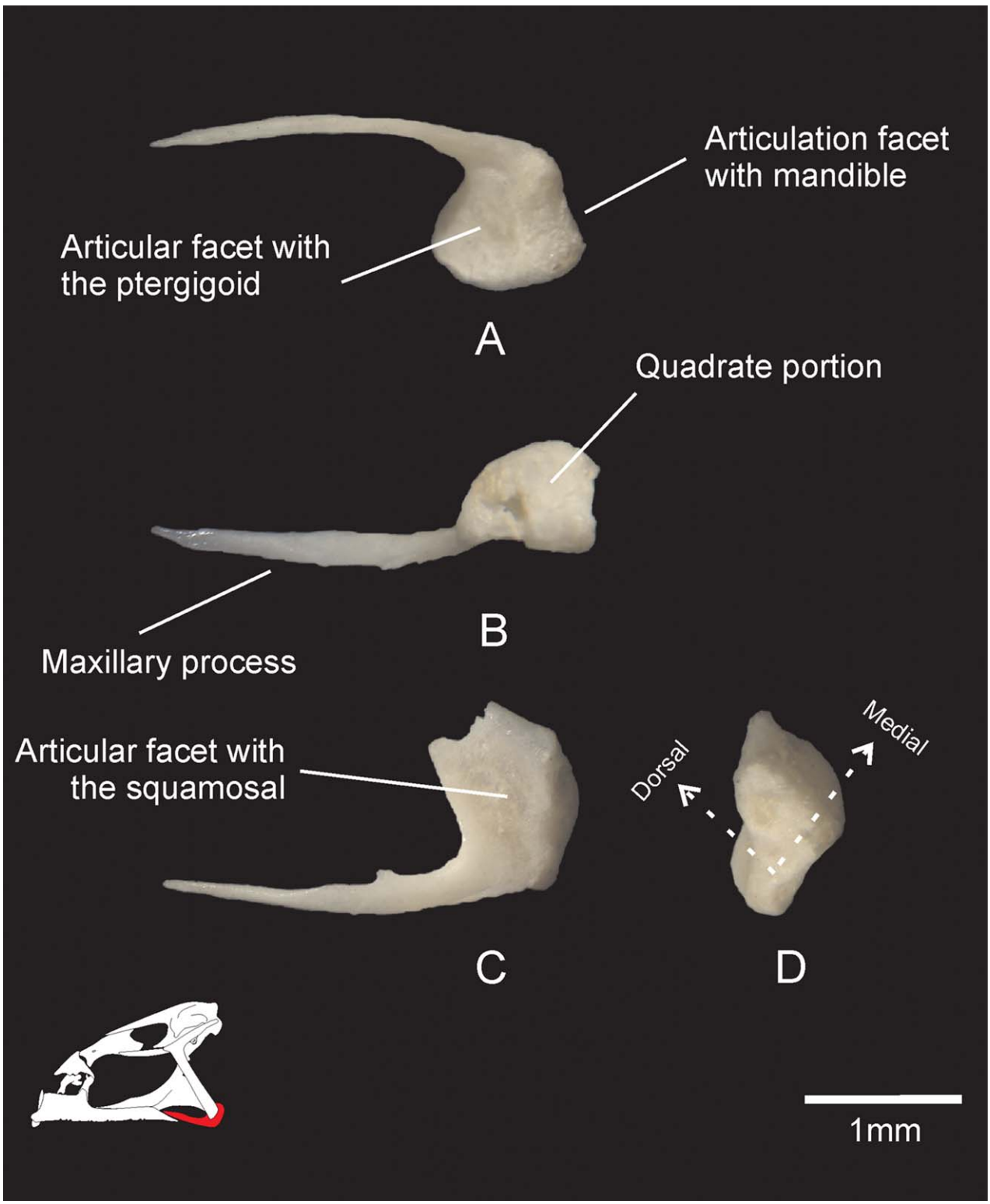

Fig. 13. Left quadratojugal of *Phyllomedusa sauvagii*: (**A**) ventromedial, (**B**) dorsomedial, (**C**) dorsolateral, and (**D**) posterior views. In A, B, and C, anterior to the left; in D, the arrows indicate the physiological directions.

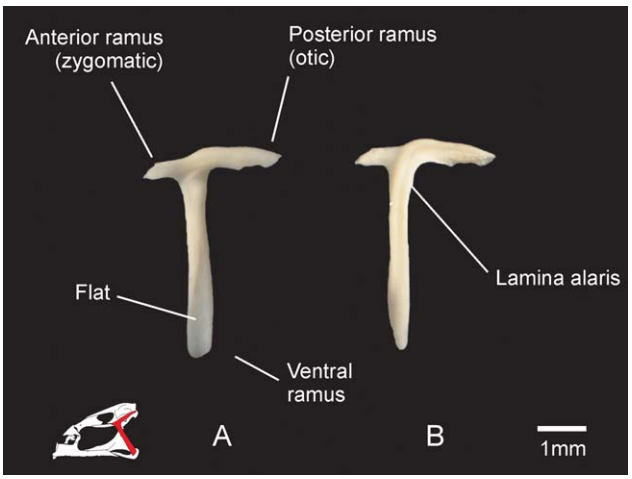

Fig. 14. Left squamosal of *Phyllomedusa sauvagii*: (**A**) lateral and (**B**) medial views. Anterior to the left.

Hyobranchial apparatus. The apparatus is formed by a central corpus, from which projects the hyalia anteriorly, and the posterlateral, and the ossified posteromedial processes (Fig. 21). The corpus is cartilaginous, quadrangular, and roughly equivalent in length and width. The U-shaped hyglossal sinus is also approximately equal in length and width. The irregular cartilaginous hyalia are very thin and project anteriorly from the anterolateral margins of the corpus hyoid; each hyale ends as a cartilaginous plate between the medial ramus of the pterygoid and the prootic. The alary processes of the hyoid are poorly developed, and present as lateral triangular swellings at the base of the hyalia; there are no anterolateral processes. Each posterolateral process is relatively short, reaching up the proximal tip of the posteromedial process; they have a medial constriction and swollen distal heads. The posteromedial processes are large and well ossified, and they are divergent at an angle of about 70°; their bases are close but not touching. Their length is similar to that of the hyoid corpus. The proximal and distal ends of the posteromedial processes are wider, whereas the shafts are narrower.

DISCUSSION

The study of the disarticulated bones has proven to be complex, yet enlightening, as there are bones such as the sphenethmoid, or areas like the internal face of the occipital complex, of which little are known in the articulated skull.

Comparison with Other Species of *Phyllomedusa*

The only descriptions of skulls detailed enough for valuable comparison with our data are those of *Phyllomedusa vaillantii* and *P. atelopoides* (Sheil and Alamillo, 2005), and *P. venusta* (Cannatella, 1980). We will not compare our data with some other skull descriptions of former *Phyllomedusa* species (as Cannatella, 1982; da Cruz, 1990) since those are now included in different genera. The general shape of the adult skull of *P. sauvagii* more closely resembles that of the *P. vaillantii* and *P. venusta*, in which the skulls are longer than they are wide. The surface of the skull of *P. sauvagii* is smooth and lacks the frontopatietal ornamentation characteristic of *P. atelopoides*, whose skull has a more equivalent length-to-width ratio. Nevertheless, when analyzing the shape of the tip of the snout, *P. sauvagii* is more similar to *P. atelopoides*, with its truncated snout, than to *P. venusta* and *P. vaillantii*, in which the snout tip is more rounded.

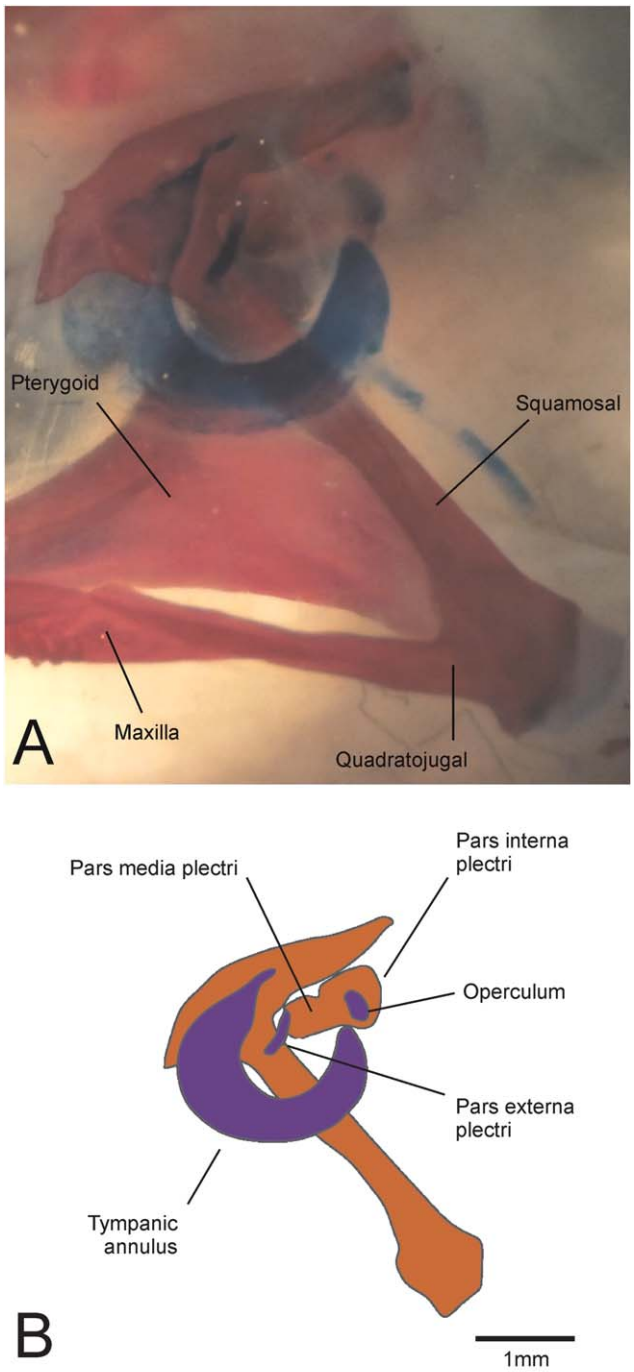

Fig. 15. Left lateral view of the auditory apparatus of *Phyllomedusa sauvagii*. Anterior to the left. In A, some bones are labeled for orientation.

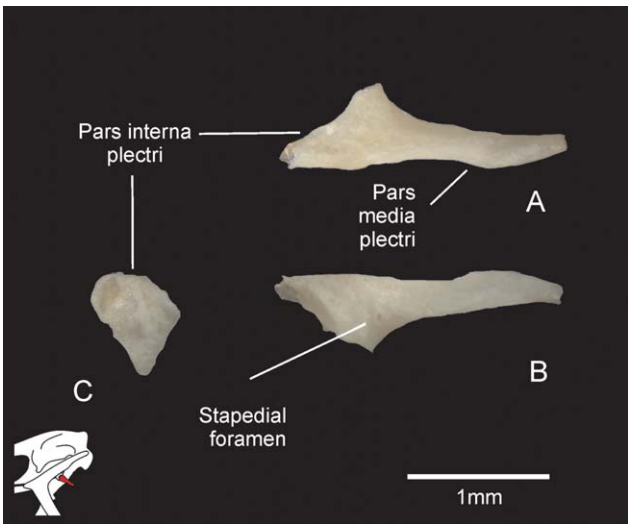

Fig. 16. The pars media plectri of the right columella of *Phyllomedusa sauvagii*: (**A**) dorsal, (**B**) ventral, and (**C**) medial views. In A and B, medial to the left.

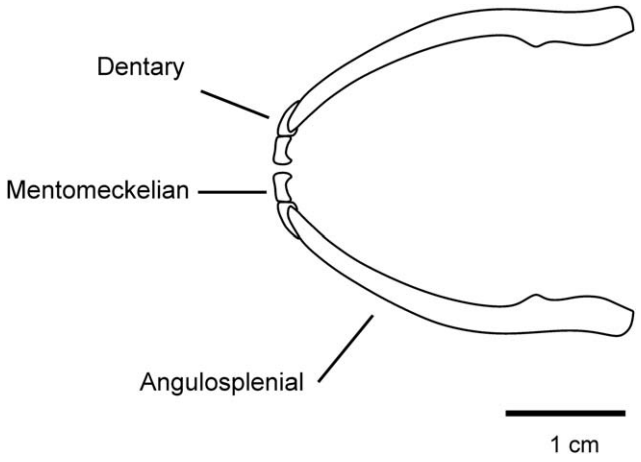

Fig. 17. Dorsal view of the mandibles of *Phyllomedusa sauvagii*. Anterior to the left.

In frontal view, the alary process of the premaxilla in *P. sauvagii, P. vaillantii*, and *P. atelopoides* does not exhibit a lateral process in comparison with other hylids (such as *Trachycephalus* and *Hypsiboas*), in which the process is present (pers. obs.). In lateral view, the alary process of the premaxilla in *P. atelopoides* is vertical, whereas in *P. sauvagii* and *P. vaillantii*, it is tilted posteriorly. The posterolateral process of the premaxilla, best noted in ventral view, is smaller than the posteromedial process in *P. sauvagii* and *P. atelopoides*, whereas it is about the same size in *P. vaillantii*.

The ventral border of the maxilla is straight in *P. sauvagii* and *P. vaillantii*, but ventrally curved in *P. atelopoides*. The articulation between the posterior process of the maxilla and the quadratojugal is very short in *P. atelopoides*, whereas in *P. vaillantii* and *P. sauvagii*, it overlaps half the length of the quadratojugal.

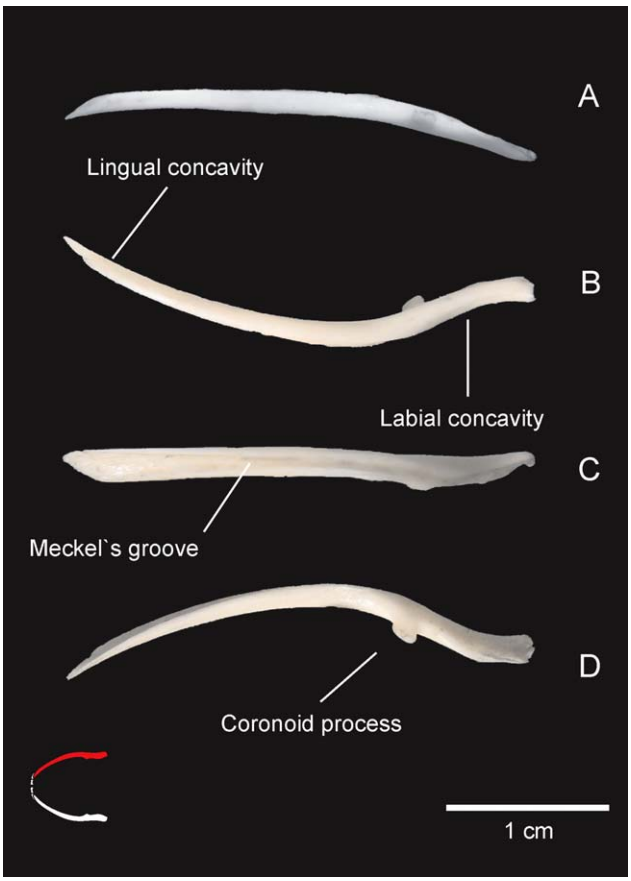

Fig. 18. Right angulosplenial of *Phyllomedusa sauvagii*: (**A**) dorsal, (**B**) medial, and (**C,D**) ventral views. Anterior to the left.

Fig. 19. Left dentary of *Phyllomedusa sauvagii* in labial (i.e., lateral) view. Anterior to the left.

The nasals of *P. atelopoides* are bigger and closer to the sagittal plane, whereas in *P. sauvagii* and *P. venusta*, the nasals are relatively smaller and have a larger gap between them. The nasals of *P. sauvagii* are peculiar in relation to the other species in that they have a very long paraorbital process.

The sphenethmoid is prominent in all four species although its shape in the articulated skull varies. In *P. atelopoides* it is rectangular in dorsal view and connected by an irregular suture to the frontoparietal; it is smaller than in the other species, and ventrally the

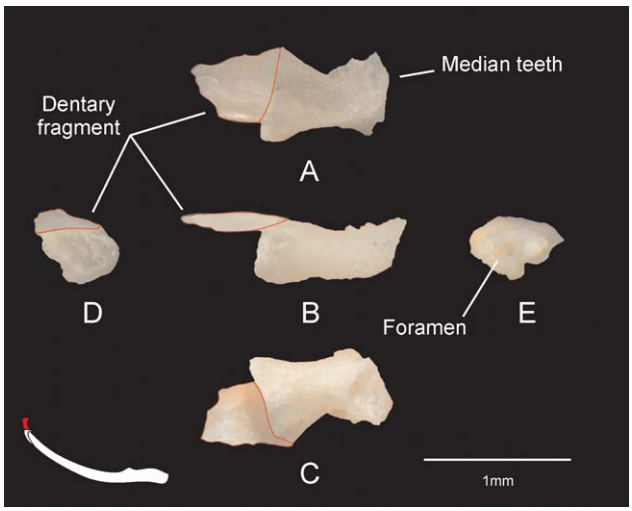

Fig. 20. Mentomeckelian bone of *Phyllomedusa sauvagii*: (**A**) labial (anterior), (**B**) dorsal, (**C**) lingual (posterior); (**D**) lateral, and (**E**) medial views. A, B, and C lateral to the left. Note the anterior part of the dentary (red) fused with the mentomeckelian bone.

posterior processes of the bone are cartilaginous (also present in *P. sauvagii*, although narrower). *Phyllomedusa vaillantii* differs from *P. sauvagii*, in that it exhibits a pair of anterior projections between the nasals, and the posterior processes are ossified. *Phyllomedusa venusta* has a longer sphenethmoid, which extends posteriorly to the midpoint of the orbit.

In *P. atelopoides*, the otic ramus of the squamosal is longer in relation to the ventral ramus than in *P. sauvagii* and *P. vaillantii*.

The vomer of *P. sauvagii* and *P. vaillantii* is robust and bears teeth; Duellman and Trueb (1967) consider this a characteristic of the *P. buckleyi* Group although it is also present in *Agalychnis aspera* and *A. granulosa* (da Cruz, 1990). On the other hand, the vomer of *P. atelopoides* is slender and lacks teeth; Caramashi (2006) consider this a characteristic of the *P. hypochondrialis* Group.

Phyllomedusa sauvagii, *P. venusta*, and *P. vaillantii* have neopalatines, which are absent in *P. atelopoides*. Those of *P. sauvagii* are longer and have sharp proximal ends, whereas in *P. vaillantii* and *P. venusta*, they are shorter and with blunt proximal ends.

In dorsal view, the frontoparietals of *P. vaillantii* and *P. venusta* are not fused at midline; in *P. sauvagii*, the posterior extreme is fused at midline and to the occipital complex, with a triangular portion that protrudes over the roof of the cranium and extends to the border of the foramen magnum. In *P. atelopoides*, they are completely fused, without fontanelle, and the posterior border of the parietal portion is straight and does not reach the foramen magnum. The size and shape of the fontanelle vary among the species: in *P. venusta*, the fontanelle is ovoid and small; in *P. vaillantii*, the posterior border is straight and narrower than the anterior; and in *P. sauvagii*, the posterior border is wavy and of the same width as the anterior. The lateral border of the frontoparietal in *P. sauvagii, P. vaillantii*, and *P. venusta* is concave and anteriorly divergent, whereas in *P. atelopoides*, it is straight and parallel.

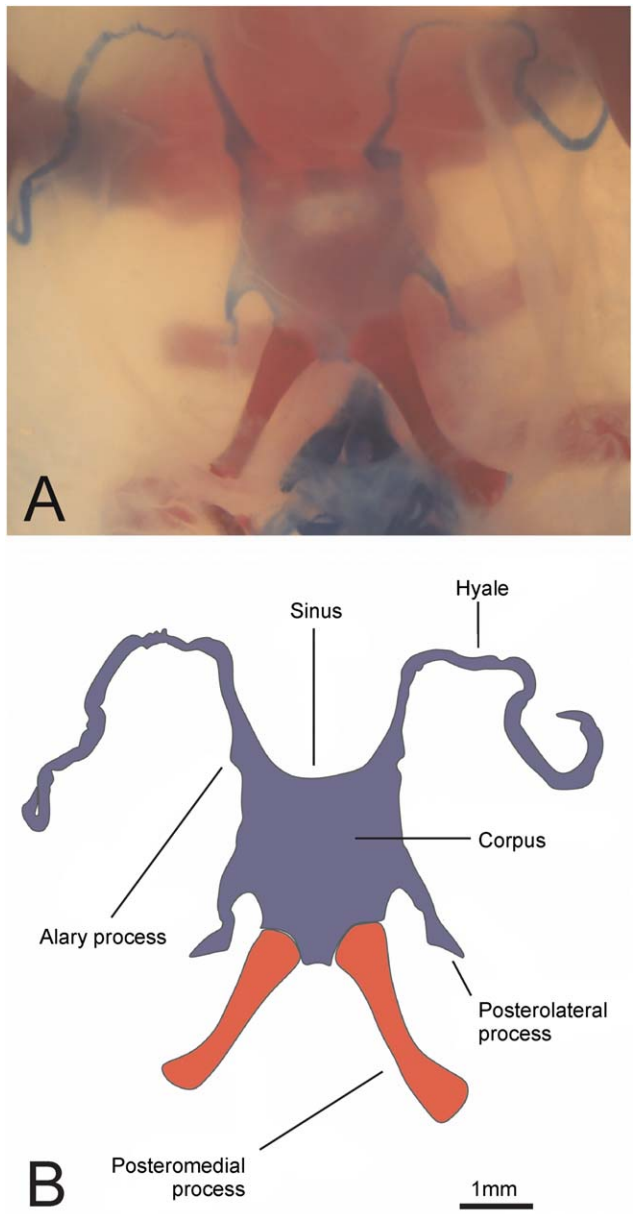

Fig. 21. Hyobranchial apparatus of *Phyllomedusa sauvagii* (FML 25331). Anterior to the top.

In the posterior region of the skull, the parotic crests of *P. sauvagii* and *P. vaillantii* are wide and separated from the squamosal by a narrow cartilage; in *P. atelopoides*, the crests are less developed and have wider cartilages.

The base of the cultriform process of the parasphenoid of *P. sauvagii* is straight, the posterolateral processes do not approach the medial ramus of the pterygoids, and the posteromedial process extends to the base of the foramen magnum. In comparison the cultriform processes of *P. vaillantii* and *P. venusta* are constrained proximally, the posterolateral processes almost touch the pterygoids, and the posteromedial process is short. In *P. atelopoides*, the base of the cultriform process is similar to that of *P. sauvagii*, but the posterolateral and posteromedial processes are relatively shorter.

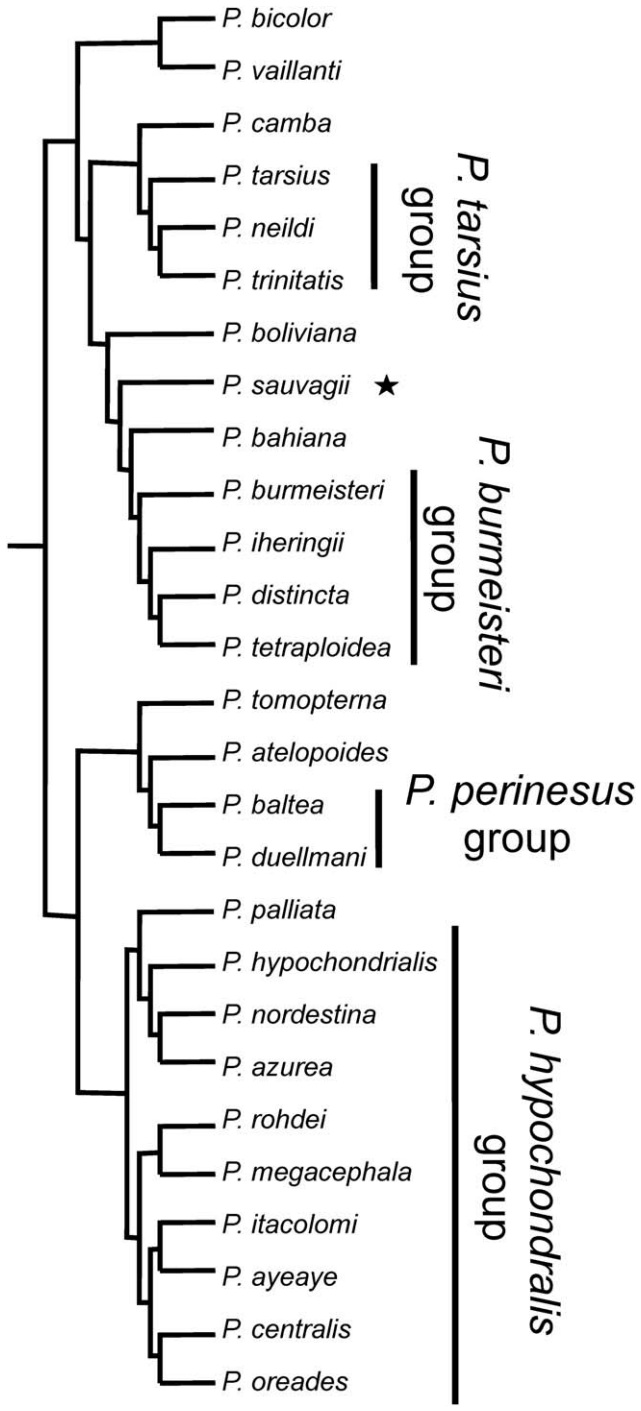

Fig. 22. Phylogeny of *Phyllomedusa* species and their putative species groups, based on Faivovich et al. (2010). *Phyllomedusa sauvagii* is indicated with a black star.

The mandibles are similar among the three species, with a few notable exceptions. The dentary forms the anterior half of the mandible in both *P. vaillantii* and *P. sauvagii*, whereas in *P. atelopoides*, it forms less than half. The anterior half of each angulosplenial bears a dorsal ridge in *P. vaillantii* and *P. sauvagii*, whereas in *P. atelopoides*, only the anterior third of each angulosplenial exhibits a dorsal ridge. Last, the coronoid process of the angulosplenial is visible in the lateral view of *P. atelopoides* and *P. sauvagii*, whereas in *P. vaillantii* it is not.

Nasal capsule. The cartilaginous structures, such as the nasal capsule, have a complex morphology and make them suitable for comparative studies. There is little research regarding the adult nasal region of most anurans as it has been predominantly studied in larval stages (e.g. de Sá and Lavilla, 1996; Haas 1996; Vera Candioti, 2007).

The nasal capsule of *P. sauvagii* is poorly chondrified in comparison with that of *P. atelopoides*, which is more extensively developed. In *P sauvagii, P. vaillantii*, and *P. atelopoides*, the nasal capsule lacks the medium prenasal process in comparison to other hylids where it is present (*Pseudacris regilla* Jurgens, 1971; *Hypsiboas pulchellus, Dendropsohus nanus, Scinax nasicus, S. fuscovarius*, and *Trachycephalus typhonius* pers. obs.).

The lateral border of the tectum nasi in *P. sauvagii* is narrow, whereas that of *P. vaillantii* and *P. atelopoides* is relatively broad. The solum nasi of *P. vaillantii* is slightly mineralized, whereas in that of *P. atelopoides* and *P. sauvagii*, it is not. The superior prenasal cartilages of *P. sauvagii* and *P. atelopoides* are thick and ovoid, and in *P. vaillantii*, they are narrower and longer. In lateral view, the anterior end of the crista subnasalis of *P. sauvagii* is taller than the posterior, whereas in *P. vaillantii*, they are the same height and, in *P. atelopoides*, they are shorter.

The superciliar cartilages of *P. sauvagii* are short and extend less than half the orbit; in comparison to *P. vaillantii* in which they are longer and extend more than half the length of the orbit. They are absent in *P. atelopoides*.

Auditory apparatus. The tympanic annulus is wider in *P. sauvagii* and *P. atelopoides* and more slender in *P. vaillantii;* the pars media plectri is osseous in *P. sauvagii* and *P. atelopoides*, whereas in *P. vaillantii*, it remains cartilaginous.

Hyobranchial apparatus. In *P. sauvagii* and *P. vaillantii*, the cartilaginous corpus of the hyoid apparatus is about as wide as it is long and the cartilaginous hyalia have irregular borders; in *P. atelopoides*, the cartilaginous corpus of the hyoid apparatus is longer than wide, and the cartilaginous hyalia are thicker than in the other species. In *P. sauvagii* and *P. atelopoides*, the corpus hiale is cartilaginous, whereas in *P. vaillantii*, it is mineralized; *P. sauvagii* exhibit alary processes, although poorly developed, whereas *P. atelopoides* and *P. vaillantii* do not.

The skull of *P. sauvagii* more closely resembles that of *P. vaillantii* than *P. atelopoides*, as *P. atelopoides* is relatively unique within the genus *Phyllomedusa*. All phyllomedusine frogs are known to be arboreal, but *P. atelopoides* is exceptional in that it is the only one that has a terrestrial life history. Because of this, it has relatively short limbs, a short, stout vertebral column, and a rather robust head, with completely fused frontoparietals (Sheil and Alamillo, 2005).

CONCLUSIONS

Of the four species discussed in this contribution, and according to Faivovich et al. (2010), *Phyllomedusa venusta* belongs to the *Phyllomedusa tarsius* species

group (Fig. 22), which putative synapomorphy is the presence of an iris with fine black reticulations. Conversely, *Phyllomedusa atelopoides, P. vaillantii*, and *P. sauvagii*, along with *P. bicolor, P. boliviana*, and *P. camba*, were historically not assigned to any species group. In that phylogeny, Faivovich et al. (2010) recovered *Phyllomedusa bicolor* and *P. vaillantii* as monophyletic, sharing the presence of osteoderms, evident as small subepidermical spines; furthermore, both taxa lack omosternum, a character state shared with other species, while *P. atelopoides* was found to be sister to the *P. perinesos* Group. In turn, *Phyllomedusa sauvagii* was recovered as a sister species of the *Phyllomedusa burmeisteri* Group and was considered a highly specialized taxon, on the basis of its reduced digital discs and the protruding parotoid glands (Funkhouser, 1957; De la Riva, 1999; Barrio-Amorós, 2006). This phylogenetic scenario provides a framework to highlight that, given the various combinations of similarities and differences among the bones of the four taxa already discussed, it is clear that the phylogenetic hypotheses presented so far do not have the last word. In fact, the osteology and chondrology of *Phyllomedusa sauvagii* skull reveal a conservative structure without exostosis or coosificaciones, in which no reductions, disappearances, or unexpected fusions (aside from the exoccipital–occipital one) are observed among the individual structures. These facts contrasts sharply with certain characteristics of adults phyllomedusines as the peculiar structure of the hindlegs (with the first toe longest than the second), its myology (especially those muscles related to the opposability of the hallux), the physiology of nitrogenous wastes (removed as urate), the variety of bioactive peptides secreted by the skin, the presence of wax glands and the associated grooming behavior, the peculiar way of building nests with leaves, the presence of transparent vesicles associated with the oocytes, to name a few. The skull structure also does not reflect the peculiarities observed in larval chondrocranium, especially the lateral expansions of the palatoquadrate and the terminal position of supra and infrarostral cartilages. The aforementioned scarcity of availabe osteological information for the genus *Phyllomedusa*, and for Phyllomedusinae in general, keeps us at the moment to make deeper discussions or conclusions.

ACKNOWLEDGEMENTS

We wish to thank Sonia Kretzschmar and Marta Cánepa for facilitating and assisting us with the specimens housed at the Herpetological Collection, Fundación Miguel Lillo. Jennifer Richardson assisted us with the English editing. We are grateful to two anonymous reviewers for making valuable suggestions on the manuscript.

LITERATURE CITED

Aquino L, Colli G, Reichle S, Silvano D, di Tada I, Lavilla E. 2015. *Phyllomedusa sauvagii*. The IUCN Red List of Threatened Species. Version 2015.2 (28 July 2015). Electronic Database accessible at www.iucnredlist.org.

Barrio-Amorós CL. 2006. A new species of *Phyllomedusa* (Anura: Hylidae: Phyllomedusinae) from northwestern Venezuela. Zootaxa 1309:55–68.

Barrionuevo JS. 2013. Osteology and postmetamorphic development of *Telmatobius oxycephalus* (Anura: Telmatobiidae) with an analysis of skeletal variation in the genus. J Morphol 274:73–96.

Bellairs AdA, Kamal AM. 1981. The chondrocranium and the development of the skull in recent reptiles. In: Gans C, Parsons TS, editors. Biology of the Reptilia, Morphology F. London. New York Academic Press. p 1–262.

Boulenger, GA. 1882. Catalogue of the Batrachia Salientia, s. Ecaudata in the Collection of the British Museum. Second Edition. London: Taylor and Francis.

Cannatella DC. 1980. A review of the *Phyllomedusa buckleyi* group (Anura: Hylidae). Occ Pap Mus Nat Hist Univ Kansas 87:1–40.

Cannatella DC. 1982. Leaf frogs of the *Phyllomedusa perinesos* group (Anura: Hylidae). Copeia 501–513. 1980

Cannatella DC. 1985. A Phylogeny of Primitive Frogs (Archaeobatrachians). Ph. D. [dissertation], University of Kansas, Lawrence.

Caramashi U. 2006. Redefinição do grupo de *Phyllomedusa hypochondrialis*, com redescrição de *P. megacephala* (Miranda-Ribeiro, 1926), revalidação de *P. azurea* Cope, 1862, e descrição de uma nova espécie (Amphibia, Anura, Hylidae). Arq Mus Nac 64:159–179.

Conrad JL. 2004. Skull, mandible, and hyoid of *Shinisaurus crocodilurus* Ahl (Squamata, Anguimorpha). Zool J Linn Soc 141:399–434.

Da Cruz CAG. 1990. Sobre as relações intergenéricas de Phyllomedusinae da Foresta Atlantica (Amphibia, Anura, Hylidae). Rev Brasil Biol 50:709–727.

de Sá R, Lavilla EO. 1996. Características de la osificación craneal en *Phyllomedusa boliviana* (Anura: Hylidae). Cuad Herpetol 9: 69–73.

De la Riva I. 1999. A new *Phyllomedusa* from southwestern Amazonia (Amphibia: Anura: Hylidae). Rev Esp Herpetol 13:123–131.

Duellman WE. 1970. Hylid frogs of Middle America. Monogr Mus Nat Hist Univ Kansas 1:1–753.

Duellman WE, Trueb L. 1967. Two new species of tree frogs (genus *Phyllomedusa*) from Panama. Copeia 1967:125–131.

Estes R, Reig O. 1973. The early fossil record of frogs: a review of the evidence. In: Vial J, editor. Evolutionary Biology of the Anurans. Columbia, MO: University of Missouri Press. p 11–63.

Faivovich J, Haddad CFB, Baeta D, Jungfer KH, Alvares GFR, Brandao RA, Sheil C, Barrientos LS, Barrio-Amoros CL, Cruz CAG, Wheeler WC. 2010. The phylogenetic relationships of the charismatic poster frogs, Phyllomedusinae (Anura, Hylidae). Cladistics 26:227–261.

Felix J, Montori A. 1986. Determinación de las especies de anfibios anuros del nordeste ibérico mediante el hueso ilion. Misc Zool 10: 239–246.

Frost, DR. 2015. Amphibian species of the world: an online reference. Version 6.0 (24/07/2015). Electronic database accessible at http://research.amnh.org/herpetology/amphibia/index.html. New York, USA: American Museum of Natural History.

Funkhouser A. 1957. A review of the neotropical tree-frogs of the genus *Phyllomedusa*. Occ Pap Nat Hist Mus Stanford Univ 5:1–90.

Gomez-Mestre I, Wiens JJ, Warkentin KM. 2008. Evolution of adaptive plasticity: risk-sensitive hatching in neotropical leaf-breeding treefrogs. Ecol Monogr 78:205–224.

Haas A. 1996. Das larvale cranium von *Gastrotheca riobambae* und seine metamorphose (Amphibia, Anura, Hylidae). Naturwiss Vereins Hamburg N F 36:33–162.

Jurgens JD. 1971. The morphology of the nasal region of Amphibia and its bearing on the phylogeny of the group. Ann Univ Stell 646:1–146.

Montero R, Gans C. 1999. The head skeleton of *Amphisbaena alba* Linnaeus. Ann Carnegie Mus 68:16–80.

Pugener LA, Maglia AM. 2007. Skeletal morphology and development of the olfactory region of *Spea* (Anura: Scaphiopodidae). J Anat 211:754–768.

Pyron RA, Wiens JJ. 2011. A large-scale phylogeny of Amphibia including over 2,800 species, and a revised classification of extant frogs, salamanders, and caecilians. Mol Phylogenet E 61:543–583.

Sanchíz B. 1998. Salientia. In: Wellnhofer P, editor. Encyclopedia of Paleoherpetology 4. Friedrich Pfeil Verlag. München. p 1–275.

Sheil CA, Alamillo H. 2005. Osteological and skeletal development of *Phyllomedusa vaillanti* (Anura: Hylidae: Phyllomedusinae) and a comparison of this arboreal species with a terrestrial member of the genus. J Morphol 265:343–368.

Trueb L. 1973. Bones, frogs, and evolution. In: Vial JL, editor. Evolutionary Biology of the Anurans: Contemporary Research on Major Problems. University of Missouri Press, Columbia p 65–132.

Trueb L. 1993. Patterns of cranial diversity in Lissamphibia. In: Hanken J, Hall BK, editors. The skull: Patterns of Structural Diversity (Vol. II). Chicago: The University of Chicago Press. p 255–343.

Vaira M, Akmentins M, Attademo M, Baldo D, Barrasso D, Barrionuevo S, Basso N, Blotto B, Cairo S, Cajade R, Céspedez J, Corbalán V, Chilote P, Duré M, Falcione C, Ferraro D, Gutierrez FR, Ingaramo M, Junges C, Lajmanovich R, Lescano J, Marangoni F, Matinazzo L, Marti R, Moreno L, Natale G, Pérez Iglesias JM, Peltzer P, Quiroga L, Rosset S, Sanabria E, Sanchez L, Schaefer E, Ubeda C, Zaracho V. 2012. Categorización del estado de conservación de los anfibios de la República Argentina. Cuad Herpetol 26:131–159.

Vera Candioti MF. 2007. Anatomy of anuran tadpoles from lentic water bodies: systematic relevance and correlation with feeding habits. Zootaxa 1600:1–175.

Wassersug RJ. 1976. A procedure for differential staining of cartilage and bone in whole formalin fixed vertebrates. Stain Technol 51:131–134.

Wiens JJ, Fetzner JW, Parkinson CL, Reeder TW. 2005. Hylid frog phylogeny and sampling strategies for speciose clades. Syst Biol 54:719–748.

Wiens JJ, Graham CH, Moen DS, Smith SA, Reeder TW. 2006. Evolutionary and ecological causes of the latitudinal diversity gradient in hylid frogs: treefrog trees unearth the roots of high tropical diversity. Am Nat 168:579–596.

Wiens JJ, Kuczynski CA, Hua X, Moen DS. 2010. An expanded phylogeny of treefrogs (Hylidae) based on nuclear and mitochondrial sequence data. Mol Phylogenet E 55:871–882.

APPENDIX 1

All specimens are housed in the herpetological collection at Fundación Miguel Lillo (FML), Tucumán, Argentina.

Specimens examined, articulated dried skulls: FML 00823, female, Tucumán. Trancas; FML 01078, male, Formosa, Matacos; FML 01097, male, Formosa, Matacos; FML 03818 – 1, male, Tucumán, San Miguel de Tucumán; FML 03818 – 2, male. Tucumán, San Miguel de Tucumán; FML 03819 – 1, male, Santiago del Estero, Figueroa; FML 03819 – 2, female, Santiago del Estero, Figueroa; FML 03820, female, Tucumán, San Miguel de Tucumán; FML 03821, male, Tucumán, San Miguel de Tucumán; FML 04724, male, Tucumán, Tafí Viejo; FML 23831, female, Tucumán. Yerba Buena; FML 25329, male, Tucumán. Yerba Buena.

Specimens examined, disarticulated dried skulls: FML 25331, male, Tucumán. Yerba Buena; FML 25334, male, Tucumán. Yerba Buena.

Specimens examined, cleared-and-double-stained specimens: FML 03812, male, Tucumán, San Miguel de Tucumán; FML 03823, female, Tucumán, San Miguel de Tucumán; FML 25330, male, Tucumán. Yerba Buena; FML 25332, male, Tucumán. Yerba Buena; FML 25333, male, Tucumán. Yerba Buena.